Article

Cu(I) Complexes of Multidentate *N,C,N*- and *P,C,P*-Carbodiphosphorane Ligands and their Photoluminescence

Marius Klein [1], Nemrud Demirel [1], Alexander Schinabeck [2], Hartmut Yersin [2], Jörg Sundermeyer *[,1]

[1] Fachbereich Chemie and Wissenschaftliches Zentrum für Materialwissenschaften, Philipps-Universität Marburg, Hans-Meerwein-Straße 4, 35043 Marburg, Germany
[2] Institute for Physical Chemistry, University of Regensburg, 93040 Regensburg, Germany
* Correspondence: J.S.: jsu@staff.uni-marburg.de.

Abstract: A series of dinuclear copper(I) *N,C,N*- and *P,C,P*-carbodiphosphorane (CDP) complexes using multidentate ligands CDP(Py)$_2$ (**1**) and (CDP(CH$_2$PPh$_2$)$_2$ (**13**) have been isolated and characterized. Detailed structural information was gained by single crystal XRD analyses of nine representative examples. The common structural motive is the central double ylidic carbon atom with its characteristic two lone-pairs involved into binding of two geminal L-Cu(I) fragments at Cu-Cu distances in the range 2.55 – 2.67 Å. In order to enhance conformational rigidity within the characteristic Cu-C-Cu triangle, two types of chelating side arms were symmetrically attached to each phosphorus atom: two 2-pyridyl functions in ligand CDP(Py)$_2$ (**1**) and its dinuclear copper complexes **2-9** and **11**, as well as two diphenylphosphinomethylene functions in ligand CDP(CH$_2$PPh$_2$)$_2$ (**13**) and its di- and mononuclear complexes **14**-**18**. Neutral complexes were typically obtained via reaction of **1** with Cu(I) species CuCl, CuI, and CuSPh or via salt elimination reaction of [(CuCl)$_2$(CDP(Py)$_2$] (**2**) with sodium carbazolate. Cationic Cu(I) complexes were prepared upon treating **1** with two equivalents of [Cu(NCMe)$_4$]PF$_6$, followed by the addition of either two equivalent of an aryl phosphine (PPh$_3$, P(C$_6$H$_4$OMe)$_3$) or one equivalent of a bisphosphine ligands DPEPhos, XantPhos or dppf. For the first time carbodiphosphorane CDP(CH$_2$PPh$_2$)$_2$ (**13**) could be isolated upon treating its precursor [CH(dppm)$_2$]Cl (**12**) with NaNH$_2$ in liquid NH$_3$. A protonated and a deprotonated derivative of ligand **13** were prepared and their coordination was compared to neutral CDP ligand **13**. NMR analysis and DFT calculations reveal, that the most stable tautomer of **13** does not show a CDP (or carbone) structure in its uncoordinated base form. For most of the prepared complexes, photoluminescence upon irradiation with UV light at room temperature was observed. Quantum yields (Φ_{PL}) were determined to 36% for dicationic [(CuPPh$_3$)$_2$(CDP(Py)$_2$)](PF$_6$)$_2$ (**4**) and to 60% for neutral [(CuSPh)$_2$(CDP(CH$_2$PPh$_2$)$_2$] (**16**).

Keywords: Carbodiphosphorane, Phosphorus Ylides, Pincer Ligands, Coordination Chemistry, Cu(I) complex, Photoluminescence.

1. Introduction

In 1961, hexaphenyl-carbodiphosphorane, the first carbodiphosphorane (CDP), was synthesized by Ramirez et al. [1]. Regardless to this early discovery the interest in such double ylide carbon (or carbone) compounds is still evolving. One reason for attracting interest is the bonding description of carbodiphosphoranes. Next to a classical ylide valence bond description, the bonding in carbodiphosphoranes can be decribed as a formal carbon(0) atom stabilized by two dative phosphine ligands with C-P retro dative bonding components, a model discussed earlier but quantified by a theoretical approach of Frenking and co-workers [2–6]. The central carbon atom is best described in its excited singlet (^{1}D) state [7]. It acts as an acceptor and is stabilized by the σ donating phosphine ligands. The two characteristic occupied lone pairs (HOMO and HOMO+1) centered at this carbon atom (therefore named "carbone"), are either capable to bind two metals via two σ bonds in a close

to tetrahedral configuration P_2CM_2 or one metal in a trigonal-planar P_2CM configuration via a σ- and a π dative bond of very strong π,σ-donor character [8]. For this reason, coordination chemistry of carbodiphosphoranes has experienced a renaissance [9–11]. A topic of current interest is introducing secondary ligand functions into the CDP frame: Cyclometalation with noble metals rhodium and platinum gave rise to the characterization of *C,C,C*-pincer ligand complexes with two cyclometalated phenyl rings [12–17], and ortho-directed double lithiation of hexaphenyl-carbodiphosphorane leads to lithium complexes capable to transfer the *C,C,C*-pincer ligand synthon $[CDP]^{2-}$ to any other element of the periodic table [17]. *P,C,P*-chelate complexes of a phosphine functionalized CDP ligand $CDP(CH_2PPh_2)_2$ (**13**), formally a carbone $C(dppm)_2$ (dppm = bis-diphenylphosphinomethane), were characterized, but the free ligand **13** was not isolated so far [18–24]. Only recently, complexes of 2-pyridyl functionalized *N,C,N*-carbodiphosphorane $CDP(Py)_2$ (**1**) were reported [25,26]. The isolation of the free ligand base **1** [25] enabled the synthesis of Cu(I) CPD complexes, which are discussed in this work. Cu(I) complexes [27–43] can be used as cost efficient luminescent materials, which potentially can replace highly phosphorescent Ir [44–50] or Pt [47,51–58] complexes in OLED technology. For example, OLED devices with internal quantum efficiencies of up to 100% could be realized based on the *TADF singlet harvesting* mechanism [28–31,41]. According to this mechanism, both the singlet and triplet excitons formed in an OLED emission layer can be harvested and emission occurs via the S_1 state.

Very frequently, Cu(I) complexes exhibit low-lying metal-to-ligand charge transfer (MLCT) transitions that are related to small energy separations $\Delta E(S_1 - T_1)$ between the lowest singlet S_1 and the lowest triplet T_1 state due to small HOMO-LUMO overlap. As a consequence, efficient up-intersystem crossing ($T_1 \rightarrow S_1$), also designated as reverse intersystem crossing RISC, can occur at near ambient temperature [28,41,45,59,60] thus, resulting in thermally activated delayed fluorescence (TADF). This is also related to a small transition dipole moment and, thus, a small radiative rate $k^r(S_1 \rightarrow S_0)$ [31,32]. The described CT transfer formally corresponds to oxidation of Cu(I) to Cu(II) and leads to a photo-induced structural rearrangements in the excited state(s) being connected to large Franck-Condon factors [61], and, as a consequence, to competing non-radiative relaxations. Therefore, the design of rigid structures with small reorganisation energy between ground state and excited states is essential.

While the first luminescent behaviour of a Au(I) N-heterocyclic carbene (NHC) complex was already described in 1999 [62], it took another ten years till the first photoluminescent Cu(I) NHC complexes were characterized [63] followed by further studies more recently [64–70]. In contrast to the π-acidic NHCs ligands, the π-donating CDP ligands have not yet been considered in luminescent materials. Herein, we report such luminescent Cu(I) CDP complexes, their synthesis, x-ray structure data, and PL properties. We demonstrate, that high emission quantum yields can be obtained with selected materials of this class.

2. Results

2.1 Synthesis and characterisation of *N,C,N*-CDP complexes

The *N,C,N*-carbodiphosphorane pincer ligand $CDP(Py)_2$ (**1**) was synthesized as reported previously [25] and used as a ligand in order to synthesize neutral and cationic dinuclear copper (I) complexes. Complexes **2**, **3** and **9** were conveniently prepared by stirring ligand **1** with two equivalents of the respective copper(I) salts CuX in THF at room temperature for 18 h. Moderate yields of 86% and 63% for **2** and **3**, as well as 27% for **9** were achieved in form of orange powders. Dicationic complexes **4**-**9** were prepared in a in situ two-step protocol by reaction of $CDP(Py)_2$ (**1**) with tetrakis(acetonitrile)copper(I) hexafluorophosphate (2 eq.) in THF, followed by addition of either two equivalents of monodentate triaryl phosphine or one equivalent of a bisphosphine ligand: Triphenylphosphine, tris(*o*-methoxyphenyl)phosphine, bis[(2-diphenylphosphino)phenyl] ether (DPEPhos), 4,5-bis(diphenylphosphino)-9,9-dimethylxanthene (XantPhos) and 1,1'-bis(diphenyl-phosphino) ferrocene (dppf) were chosen as ligands. The dicationic Cu(I) complexes were isolated and crystallized in yields of 47-90% (Scheme 1). Additionally, a neutral Cu(I) CDP complex was

obtained via deprotonation of carbazole (**10**) in THF using sodium *tert*-butoxide and addition of $[(CuCl)_2(CDP(Py)_2)]$ (**2**) to this solution. $[(CuCarb)_2(CDP(Py)_2)]$ (**11**) was obtained as light orange powder in a yield of 56%. Complexes **2**-**9** and **11** have been characterized via ^{31}P NMR, ^{1}H NMR, ^{13}C NMR, and by elemental analyses. Due to the typically poor volatility of ionic and zwitterionic Cu(I) complexes **2**-**9** no mass spectra with molecular ions were obtained under EI, FD and ESI ionisation techniques. However, a molecular ion of **11** (*m*/*z* 539.18016: $[M-H]^+$) could be detected by using liquid injection field desorption ionization (LIFDI) indicating the strong and proton capturing Cu-N bond between the copper(I) and the nitrogen atom of the *N*-carbazolyl anion. This strong interaction can be traced back to the C-N bond distance, which will be discussed below.

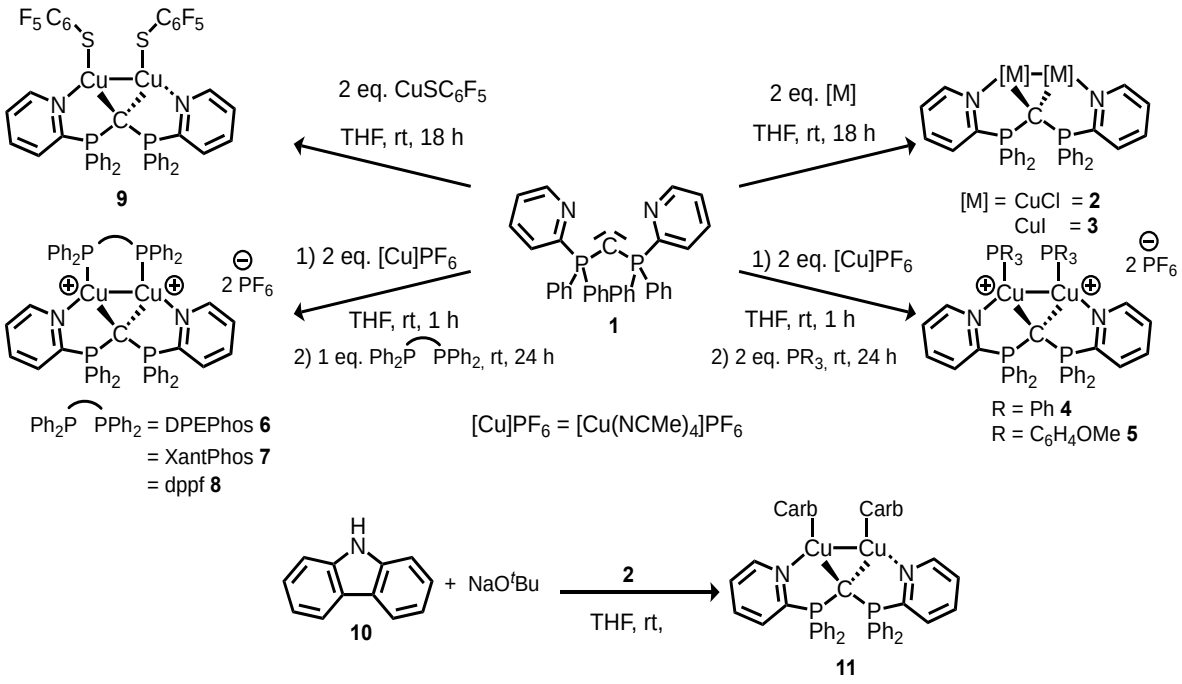

Scheme 1. Synthesis of a wide variety of novel dinuclear *N*,*C*,*N*-carbodiphosphorane complexes **2**-**9** and **11**.

Single crystals suitable for X-ray diffraction analysis were obtained upon layering THF or DCM solutions of the complexes with *n*-pentane. Crystal structures for **2**, **4**, **6**, **7**, **9**, and **11** are shown in Figure 1, selected bond distances and angles in Table 1. Further details of the XRD analyses of **3**, **5** and **8** are described in the Supporting Information. The molecular structures of **2**-**9** reveal, that the central carbon atom within the CDP ligand is capable of coordinating two copper atoms in a geminal fashion. Each copper atom is additionally coordinated by one 2-pyridyl unit of ligand **1**. If the Cu-Cu interaction is disregarded the two copper atoms per molecule are coordinated in a planar fashion, more T-shaped than trigonal planar. Each copper atom is interacting with one of the two carbone lone pairs of the central carbon atom C1, each by one nitrogen atom of a 2-pyridyl chelate ring and by the variable neutral ligand L or anionic ligand X. The strongest ligand interactions (C and X/phosphine) define a Cu(I) archetypical close to linear axis. The geminal nature of both copper(I) centers leads Cu-Cu distances in the range 2.55 – 2.67 A° (Table 1). These distances are smaller than twice the size of the covalent radius of Cu (1.32 Å) [71] or twice the size of the van der Waals radius of Cu (1.4 Å) [72]. Twice the size of the Cu(I) covalent radius (1.27 Å) [73] is close to the observed Cu-Cu distance. Similar trends are observed in dinuclear Cu(I) CDP complexes without any constraints of additional chelating CDP functions [74]. The Cu-Cu interaction leads to a formally coordinatively saturated pseudo tetrahedral coordination around each copper atom. This dinuclear entity is intramolecularly stabilized by a neutral 4-electron donor carbone ligand bridging the two Cu atoms. This rather rigid ligand template is characterized by characteristic torsion angles X-Cu-Cu-X in the range 41.9 ° (**2**) – 76.0 ° (**3**) for anionic ligands X (X = Cl, I, $S(C_6F_6)$ or L-Cu-Cu-L in the range 62.4 ° (**8**)

– 82.9 ° (**4**) for phosphine and the bridging bisphosphine ligands. The rather rigid frame of this *N,C,N*-ligand backbone seems to be privileged to stabilize this 8-electron-5-center inner Cu_2CN_2 core.

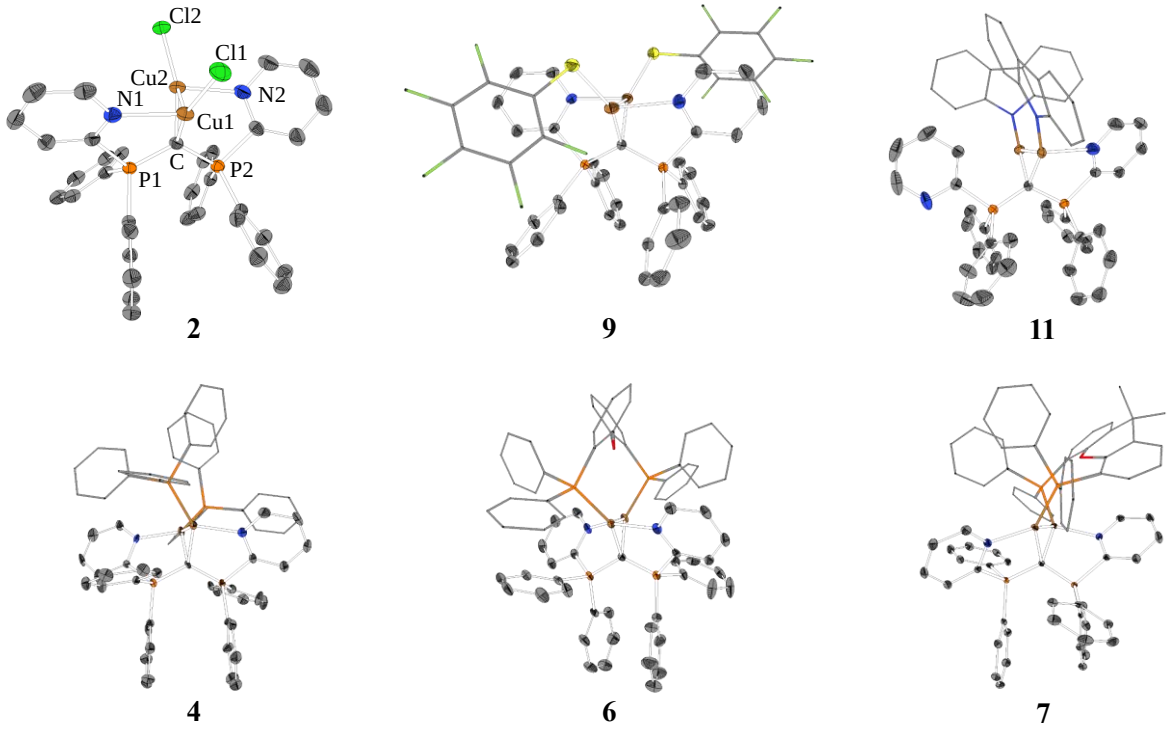

Figure 1. XRD molecular structures of $[(CuCl)_2(CDP(Py)_2)]$ (**2**), $[Cu_2(PPh_3)(CDP(Py)_2)](PF_6)_2$ (**4**), $[Cu_2(DPEPhos)(CDP(Py)_2)](PF_6)_2$ (**6**), $[Cu_2(XantPhos)(CDP(Py)_2)](PF_6)_2$ (**7**), $[(CuS(C_6F_5))_2(CDP(Py)_2)]$ (**9**) and $[(CuCarb)_2(CDP(Py)_2)]$ (**11**). Hydrogen atoms and solvent molecules have been omitted for clarity; thermal ellipsoids are given at 50% probability. For details and further XRD molecular structures of **3**, **5** and **8** see the Supporting Information.

Representative parent complex **2** crystalizes in a triclinic crystal system with a crystallographic point group of *P*-1 and with four units and two unique molecules in the unit cell. One of the two independent molecules is slightly disordered, both have very similar geometric parameters. The angles (°) around copper are almost identical for the two Cu atoms, but crystallographically not strictly identical: C-Cu-Cl 162.11(8) °, C-Cu-N 89.45(9) ° and N-Cu-Cl 106.95(6) °.Each copper atom deviates only marginally from the plane defined by C, N and X = Cl to which copper(I) is bound. Cu-Cu distances, which indicate weak Cu-Cu interactions, e.g. 2.5525(5) Å for **2**. The C-Cu-Cu angles of 2 and related species are typically sharp, e.g. 49.98(7) ° in case of **2**. A comparable coordination scenario can be found for the other complexes **3**-**9**. Only small differences for the C-P distances as well for the Cu-C-Cu and the P-C-C angles are observed within the series **2**-**9**.

Table 1. Selected bond distances [Å] and angles [°] for **2**-**9** and **11**.

	Cu-Cu	C-P1	C-P2	Cu-X[1]	Cu-C-Cu	P1-C-P2
2	2.5525(5)	1.714(3)	1.718(2)	2.1504	80.26(9)	121.51(14)
3	2.5727(10)	1.679(5)	1.702(5)	2.4501	78.64(19)	128.5(3)
4	2.6039(16)	1.709(10)	1.693(9)	2.186	79.3(3)	126.8(6)
5	2.5768(5)	1.707(3)	1.710(3)	2.2024	78.29(10)	123.64(18)
6	2.5798(6)	1.710(4)	1.712(4)	2.1903	78.77(13)	124.0(2)
7	2.5580(3)	1.7064(19)	1.7211(18)	2.1920	77.73(6)	122.10(11)
8	2.5882(16)	1.730(6)	1.717(6)	2.1915	80.0(2)	121.8(4)
9	2.6667(7)	1.710(3)	1.710(3)	2.1881	83.01(11)	123.70(17)
11	2.671(2)	1.726(2)	1.728(2)	1.886	86.14(12)	120.45(15)

[1]Average value of the distances of Cu1-X1 and Cu2-X2. X = Cl, I, S, P or N.

Complex **11** crystalizes in a monoclinic crystal system with a space group of $P2_1/n$ and four units in its unit cell. In contrast to the described XRD molecular structures of **2**-**9**, the neutral complex **11** shows only one pyridine copper interaction, the remaining pyridyl unit stays in a dangling nonbonding situation. The carbazolyl anions display a perpendicular orientation with respect to each other. Both, steric and electronic factors are probably responsible for the dangling pyridyl unit in **11**. As expected, the Cu-N_{carb} distance 1.911(3) Å for copper with the higher coordination number due to additional pyridine interaction is longer than Cu-N_{carb} 1.861(2) Å for the other one. According to NMR spectroscopy, there is a dynamic exchange process of bonded and dangling pyridine ligands in solution.

2.2 Synthesis and characterisation of *P,C,P*-CDP complexes

Peringer et al. developed *P,C,P*-CDP pincer complexes of a formal carbone ligand $C(dppm)_2$, which was not isolated and characterized, but trapped in form of its complexes [18–24]. The synthetic strategy involved complex redox reactions. It is limited to the characterisation of Ni(II), Pd(II), Pt(II) or Au(III) complexes so far. Our synthetic approach was to isolate the free CDP base. Thus, $[CH(dppm)_2]Cl$ (**12**) [18,19] was treated with an excess of sodium amide (6.5 eq.) in liquid ammonia at –78 °C. Since the basicity of sodium amide leads to deprotonation of only one proton, $CDP(CH_2PPh_2)_2$ (**13**) could be isolated in 98% yield as an intense yellow powder. No further deprotonation products and no adduct formation with lithium salts were observed as in case of using organolithium bases. The isolation of **13** was the precondition to access the coordination chemistry of Cu(I) with this *P,C,P*-CDP ligand base. Dinuclear copper complexes **14**-**16** where synthesized and characterized via NMR spectroscopy and mass spectrometry (Scheme 2). Upon treating **13** with tetrakis(acetonitrile)copper(I) hexafluorophosphate in DCM, a cationic complex $[CuCl(H\text{-}CDP(CH_2PPh_2)_2]PF_6$ (**17**) was obtained. The enhanced basicity of alkyl-substituted CDP **13** compared to pyridyl-substituted CDP **1** leads to a protonation of a lewis acid activated acetonitrile ligand. Therefore, monoprotonated **13** is acting as ligand in mononuclear copper complex **17** with hexafluorophosphate as counter ion. While searching for adequate bases for the deprotonation of **12**, we observed the ability of *n*-BuLi (2 eq.) to further deprotonate CDP **13**, generating an anionic CDP ligand **20** (Scheme 3) as lithium salt. Trapping this anion with one equivalent of tetrakis(acetonitrile)copper(I) hexafluorophosphate and one equivalent of triphenylphosphine leads to neutral copper(I) complex **18** as a light yellow powder in 73% yield. **18** was characterized via ^{31}P NMR, ^{1}H NMR and elemental and XRD analysis.

Preprints (www.preprints.org) | NOT PEER-REVIEWED | Posted: 21 July 2020 doi:10.20944/preprints202007.0490.v1

Peer-reviewed version available at Molecules 2020, 25, 3990; doi:10.3390/molecules25173990

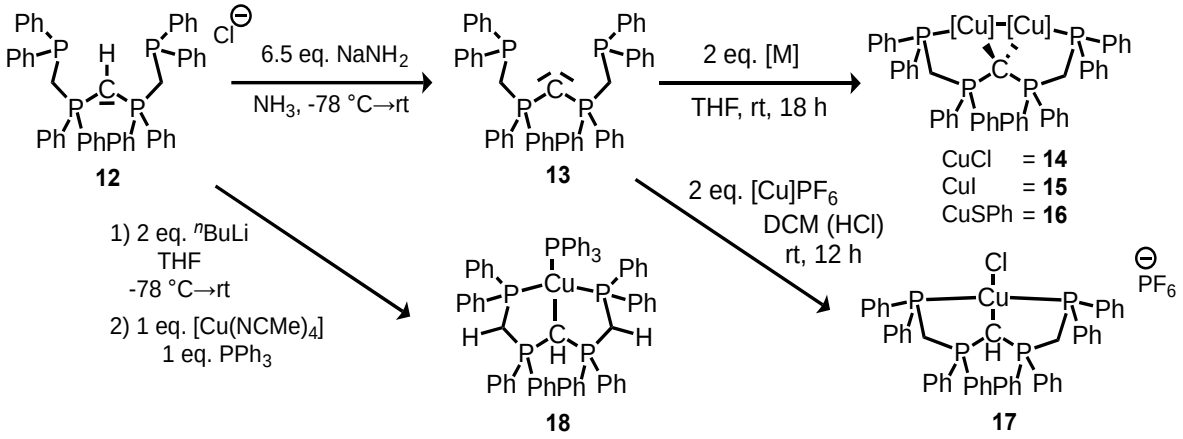

Scheme 2. Synthesis of dinuclear *P,C,P*-CDP complexes **14**-**16** via isolation of previously non-characterized $CDP(CH_2PPh_2)_2$ (**13**). A mono-protonated form of **13** was trapped and characterized in **17** and a mono-deprotonated form of **13** in **18**.

As ^{31}P NMR spectra of symmetric **12** become complex upon formation of mono-deprotonated base **13**, we anticipated the presence of tautomeric forms of **13**. Potential tautomers were investigated via computational methods (Scheme 3). Geometry optimizations were performed at the PBE-D3(BJ)/def2-TZVPP level of theory. Followed by single point calculations and a natural bond orbital (NBO) analysis at the PBE0-D3(BJ)/def2-TZVPP level of theory. Interestingly, the results reveal that the free ligand base **13** cannot be acknowledged as a carbodiphosphorane, but rather as tautomer **13a**. Due to the high first proton affinity (PA) and drastically lower second PA of the alkyl substituted central CDP carbon atom and due to the enhanced CH-acidity of the methylene group placed inbetween a phosphanyl and a phosphionio functionality, the ground state of **13** is not represented by tautomer **13c** or **13b** but by asymmetric tautomer **13a**. This equilibrium explains the highly complex ^{31}P NMR spectra obtained from solutions of pure **13**. Symmetric tautomer **13b** is 4.1 kcal/mol more stable than **13c**, but asymmetric **13a** is 7.7 kcal/mol more stable than **13b**. Our results from solution and gas phase investigation and very clear results from XRD solid state investigations of ligand **13** complexes indicate, that the equilibrium of tautomers displayed in Scheme 3 is shifted towards **13c**, if the free base **13** is trapped by coordination with two Cu(I) ions! Further deprotonation of **13a** leads to symmetric carbanion **20** as most stable tautomer: **20a** with equally CH-functionalized C1, C2 and C3 is 12.7 kcal/mole more stable than asymmetric tautomer **20b** retaining a carbodiphosphorane structure. A hypothetical $1\lambda^5,3\lambda^3$ diphosphete derivate **20c** is just 1.1 kcal/mole less stable than **20b** in the gas phase. The charge distribution of the tautomers can be monitored via NBO analysis. While the atomic partial charge q(C) of C1 of **13a** is −1.38 e, which corresponds to q(C) of the protonated hexaphenyl-carbodiphosphorane (−1.33 e) [6]; the one of **13c** reveals as −1.45 e and therefore is in the same order of magnitude as for the hexaphenyl-carbodiphosphorane (−1.43 e) [6]. For **20a** q(C) of C1, C2 and C3 are -1.39 e, 1.37 e and 1.37 e, while q(C) of P1, P2, P3 and P4 are 1.68 e, 1.68 e, 0.83 e and 0.83 e. For more information regarding the atomic partial charges and for a detailed deprotonation of **12** see Table S1-S8, as well as Scheme S-1 in the SI.

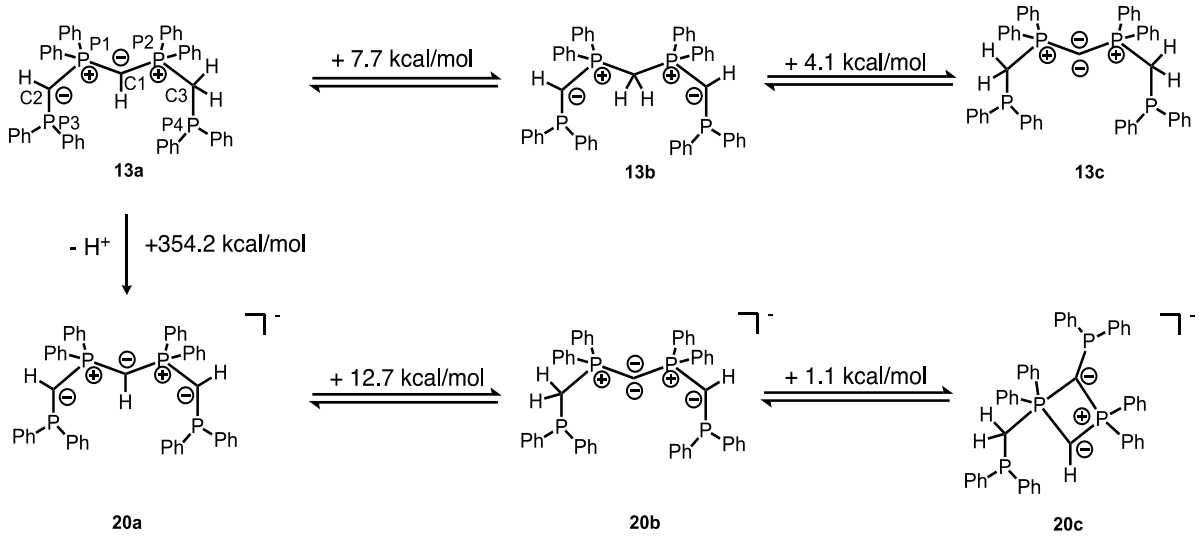

Scheme 3. Results of quantum chemical calculations on the deprotonation of [H-CDP(CH_2PPh_2)$_2$]Cl (**12**) and formation of different more or less stable tautomers of CDP(CH_2PPh_2)$_2$ (**13**). The positive value of the energy corresponds to the energy that has to be applied in order to convert one molecule into the other. The most stable tautomer **13a** and its deprotonation product **20a** are shown on the left side of the scheme.

Single crystals suitable for X-ray diffraction analysis where obtained upon layering a THF or a DCM solution of the complexes **14**-**18** with *n*-pentane. The XRD molecular structures are depicted in Figure 2, selected bond distances and angles in Table 2 and 3. For dinuclear complexes **14**-**16** a very similar trend is observed as discussed in chapter 2.1. The central CDP carbon atom acts as 4-electron donor involving two geminal copper atoms into a Cu-C-Cu triangle. Each copper atom is further coordinated to one chelating phosphine group. While **14** and **16** crystalize in a triclinic crystal system with space group *P*-1 and two units in the unit cell, **15** crystalizes in a monoclinic crystal system with space group *C*2/c and four units in the unit cell. In contrast to dinuclear Cu(I) complexes of pyridyl-CDP **1**, complexes **14**-**16** of phosphanyl-CDP **13** reveal significantly longer Cu-Cu distances (Å). 2.8681(5) (**14**), 2.8816(12) (**15**) and 2.989(2) (**16**) compared to 2.5525(5) (**2**) and 2.671(2) (**11**). This is in accord with the higher steric demand of the phosphine and an increased freedom of motion in CDP ligand **13** compared to the more rigid and compact CDP **1** (also compare the XYZ.file of the SI). In contrast to **2**-**9**, disregarding the Cu-Cu interaction, a less pronounced T-shape but more trigonal planar coordination sphere of the copper(I) ions is observed for **14**-**16**. This is probably due to the fact, that phosphines, carbones and the anions X are more similar in their donor strength and Cu(I) affinity compared to weaker pyridine ligands in the first series of compounds. For **14** the angles (°) around copper are 128.57(7) (C-Cu-Cl), 99.71(7) (C-Cu-P) and 129.61(3) (P-Cu-Cl) and therefore closer to the ideal 120 ° of a trigonal coordination sphere compared to **2**. This rather rigid ligand template is characterized by characteristic torsion angles X-Cu-Cu-X in the range 119.9 ° (**15**) – 140.2 (**16**) and are therefore larger compared to the complexes of **2**. The less rigid frame of this *P,C,P* ligand backbone stabilizes an 8-electron-5-center inner Cu_2CP_2 core.

Preprints (www.preprints.org) | NOT PEER-REVIEWED | Posted: 21 July 2020 doi:10.20944/preprints202007.0490.v1

Peer-reviewed version available at Molecules 2020, 25, 3990; doi:10.3390/molecules25173990

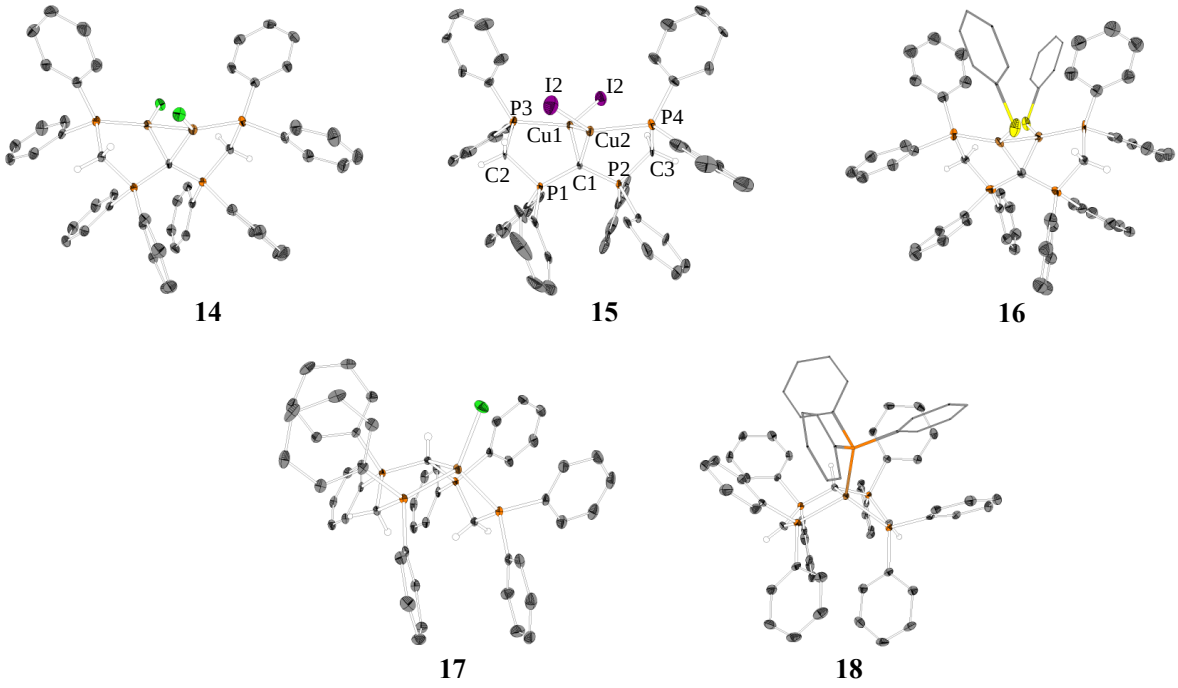

Figure 2. XRD molecular structures of $[(CuCl)_2(CDP(CH_2PPh_2)_2]$ (**14**), $[(CuI)_2(CDP(CH_2PPh_2)_2]$ (**15**), $[(CuSPh)_2(CDP(CH_2PPh_2)_2]$ (**16**), $[CuCl(H\text{-}CDP(CH_2PPh_2)_2]PF_6$ (**17**) and $[CuPPh_3(CH(PPh_2CHPPh_2)_2]$ (**18**). Hydrogen atoms and solvent molecules have been omitted for clarity; thermal ellipsoids are given at 50% probability. For more details see the Supporting Information.

Selected bond distances and angles of **14**-**16** can be found in Table 2, which demonstrates an increase of the Cu-C-Cu angle of about 10 ° in addition to the increased Cu-Cu distances relating to the increasing freedom of motion of **13** compared to **1**. The P-C-P angles of the CDP complexes **14**-**16** are comparable to the ones of ligand **1**.

Table 2. Selected bond distances [Å] and angles [°] for **14**-**16**.

	14	**15**	**16**
Cu-Cu	2.8681(5)	2.8816(12)	2.989(2)
C-P1	1.718(2)	1.716(3)	1.707(12)
C-P2	1.717(2)	1.717(2)	1.718(12)
Cu-X[1]	2.2041	2.4396(7)	2.195
Cu-C-Cu	90.02(9)	90.02(9)	92.0(4)
P1-C-P2	122.86(14)	126.3(4)	126.9(7)

[1]Average value of the distances of Cu1-X1 and Cu2-X2.

X=Cl, I or S.

Selected bond distances and angles of **17** and **18** are displayed in Table 3 and are compared to the ones of complex **14**. While $[CuCl(H\text{-}CDP(CH_2PPh_2)_2]PF_6$ (**17**) can be considered as a complex of a cationic ligand, $[CuPPh_3(CH(PPh_2CHPPh_2)_2]$ (**18**) has to be considers as an example of a complex with the deprotonated, anionic form of ligand **13**. The charge distribution of the corresponding ligand is also reflected in the C-P distances within the complexes **14**, **17** and **18**. While C1-P1 and C1-P2 are distinctly shorter for **14** an increase in C-P bond distance is observed for **17** and **18** due to the protonation of C1. Furthermore, deprotonation of C2 and C3 of complex **18** leads to a shortening of the distances C2-P1, C2-P3 and C3-P2, C3-P4 compared to **14** and **17**, where C2 and C3 are considered

as methylene groups. This also corresponds to the P1-C2-P3 and P2-C3-P4 angles, which are significantly larger for the anionic ligand complex **18** compared to **14** and **17**.

Table 3. Selected bond distances [Å] and angles [°] for **14**, **17** and **18**.

	17	**18**	**14**
C1-Cu	2.304(2)	2.196(3)	2.0275[a]
C1-P1	1.745(2)	1.761(3)	1.718(2)
C1-P2	1.745(2)	1.777(3)	1.717(2)
C2-P1	1.745(2)	1.700(3)	1.824(2)
C2-P3	1.846(2)	1.699(3)	1.846(2)
C3-P2	1.800(2)	1.742(3)	1.823(2)
C3-P4	1.847(2)	1.737(3)	1.847(2)
P3-Cu(1)	2.2588(6)	2.2774(9)	2.2649(7)
P4-Cu(2)	2.2629(6)	2.2767(9)	2.2701(7)
Cu-X	2.2753(6)	2.2509(9)	2.204[a]
P1-C1-P2	125.26(14)	124.26(17)	122.86(14)
P1-C2-P3	107.70(12)	115.90(19)	108.03(12)
P2-C3-P4	109.53(12)	120.13(18)	108.17(12)
P3-Cu-P4	113.07(2)	116.76(3)	—
C1-Cu-P3	94.80(6)	95.17(8)	99.71(7)
C1-Cu-P4	94.87(6)	94.41(8)	98.92(7)
C1-Cu-X	108.08(6)	118.49(3)	129.95[a]
P3-Cu-X	118.72(2)	113.48(8)	129.61(3)
P4-Cu-X	120.21(2)	113.87(3)	127.98(3)

X=Cl or P. [a]Average value of the distances.

2.3 Photophysical characterisation of selected CDP complexes

Since photophysical properties of carbodiphosphorane Cu(I) complexes have not yet been considered, first investigations were performed in this report. The Cu(I) complexes **2**-**7**,**9** and **14**-**16** show photoluminescence upon irradiation with UV light at room temperature. As proof of concept, we investigated emission spectra and quantum yields of $[(CuPPh_3)_2(CDP(Py)_2)](PF_6)_2$ (**4**) and $[(CuSPh)_2(CDP(CH_2PPh_2)_2]$ (**16**). Figure 3 illustrates the normalized room-temperature emission spectra of these materials. Compound **4** shows an emission maximum at 541 nm, corresponding to green/yellow color, along with a quantum yield (Φ_{PL}) of 36% for the powder sample. The emission maximum of $[(CuSPh)_2(CDP(CH_2PPh_2)_2]$ (**16**) (powder) is found at 510 nm (green color) showing Φ_{PL} = 60%. The high quantum yields indicate relatively high rigidity of the complexes in powder form. Moreover, these materials are chemically robust: After exposing the complexes to air for two months, the compounds still show their characteristic photoluminescence upon irradiation with UV light at room temperature.

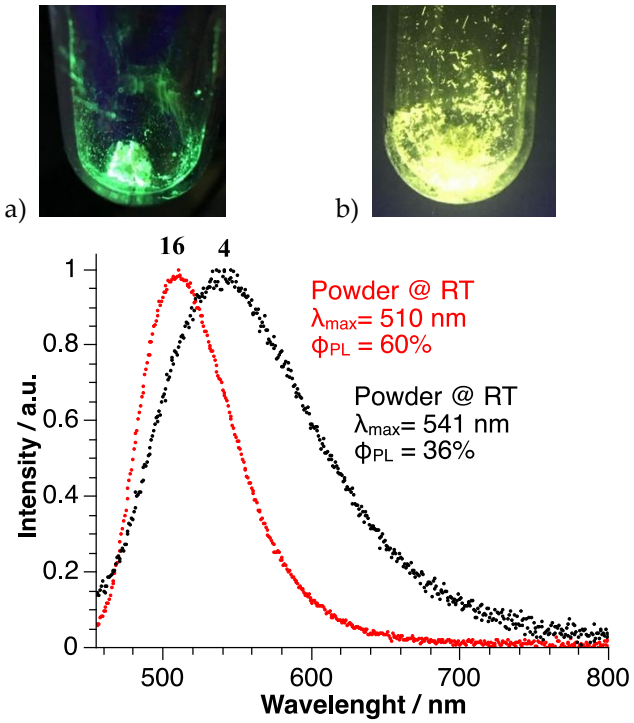

Figure 3. Normalized room-temperature emission spectra for $[(CuPPh_3)_2(CDP(Py)_2)](PF_6)_2$ (**4**) and $[(CuSPh)_2(CDP(CH_2PPh_2)_2]$ (**16**). a) illustrates the photoluminescence upon irradiation with UV light at room temperature of **16**, b) of complex **4**.

First insight in the electronic structure of the emitting compounds **4** and **16** is obtained from consideration of the HOMO and LUMO distributions. Figure 4 shows that the HOMO shows for both compounds significant participation of metal d character as well as a marginal contribution of the central carbon. The LUMO, on the other hand, is primarily localized at the pyridyl units of the ligand backbone as well as on the phenyl groups attached to P1 and P2 for **16**. Considering HOMO→LUMO transitions, the excitations can be ascribed to metal-to-ligand charge transfer (MLCT) transitions. Accordingly, it is indicated that the energy separations $\Delta E(S_1 - T_1)$ between the lowest singlet S_1 and triplet T_1 states are small enough to allow for up-ISC at ambient temperature [28,31,32]. Therefore, we tentatively assign the emission observed as TADF emission. Details will be reported in a subsequent study.

For completeness, it is mentioned that also complexes **17** and **18** exhibit photoluminescence upon irradiation with UV light at room temperature. This was not the case for $[Cu_2(dppf)(CDP(Py)_2)](PF_6)_2$ (**8**) and $[(CuCarb)_2(CDP(Py)_2)]$ (**11**). For **8**, quenching of the ferrocenyl ligand could be responsible for the lack of photoluminescence. In case of **11**, a reason could be the asymmetric coordination found in the crystal structure. The reduced rigidity could lead to larger geometry rearrangement after excitation and thus, to quenching.

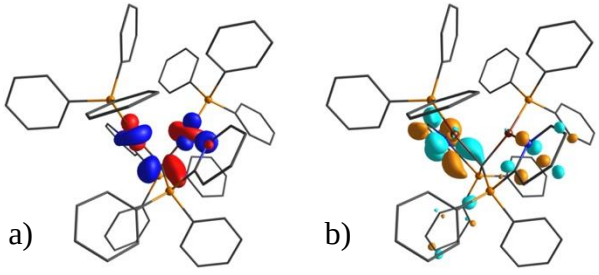

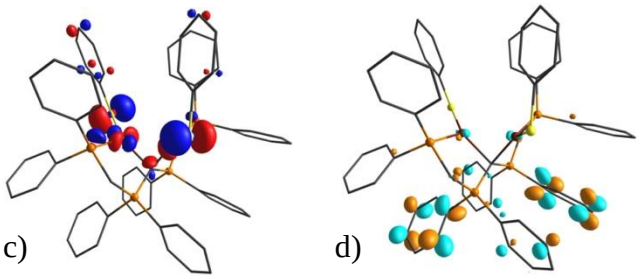

Figure 4. Kohn-Sham orbitals of HOMO (a), LUMO (b) of $[(CuPPh_3)_2(CDP(Py)_2)](PF_6)_2$ (**4**) and HOMO (c), LUMO (d) of $[(CuSPh)_2(CDP(CH_2PPh_2)_2]$ (**16**) calculated for the optimized S_0 state geometry (isovalue = 0.05). Calculations were performed at the PBE-D3(BJ)/def2-TZVPP level of theory. For more details of the MOs compare Figure S-42 and Figure S-43 in the supplement.

3. Conclusion.

We successfully isolated and characterized a series of dinuclear copper(I) complexes of two so far poorly investigated, multidentate pyridyl and phosphanyl functionalized *N,C,N-* and *P,C,P-*carbodiphosphorane ligands. A series of neutral complexes of $CDP(Py)_2$ (**1**) with anionic coligands X and a series of dicationic complexes with monodentate and bridging bidentate bisphosphine ligands DPEPhos, XantPhos, dppf were fully characterized including their XRD molecular structures. In order to prepare unprecedented dinuclear copper complexes with a previously discovered *P,C,P-*carbodiphosphorane ligand backbone, it was necessary to isolate the free ligand base $CDP(CH_2PPh_2)_2$ (**13**), which has not been demonstrated before. **13** can be obtained from $[CH(dppm)_2]Cl$ (**12**) and an excess of sodium amide in liquid ammonia. DFT calculations reveal, that the ground state of **13** has no CDP structure in the gas phase, but rather an unsymmetric tautomer form **13a**. However, upon reaction with CuX, the CDP tautomer is trapped from the tautomeric equilibrium and neutral dinuclear Cu(I) CDP complexes are isolated and fully characterized. In addition, a protonated and a deprotonated ligand form of **13** were characterized in mononuclear complexes $[CuCl(H\text{-}CDP(CH_2PPh_2)_2]PF_6$ (**17**) and $[CuPPh_3(CH(PPh_2CHPPh_2)_2]$ (**18**). With exception of $[Cu_2(dppf)(CDP(Py)_2)](PF_6)_2$ (**8**) and $[(CuCarb)_2(CDP(Py)_2)]$ (**11**)) the complexes studied show photoluminescence upon irradiation with UV light at room temperature. Photophysical measurements reveal quantum yields Φ_{PL} of 36% and 60% for $[(CuPPh_3)_2(CDP(Py)_2)](PF_6)_2$ (**4**) and $[(CuSPh)_2(CDP(CH_2PPh_2)_2]$ (**16**). As found in the crystal structure, the formal central carbon(0) atom is capable of coordinating two copper atoms relatively close two each other. They are further coordinated in a chelating manner to the chelating side arms of the CDPs. This rigid ligand design leads to high emission quantum yields and makes the CDP complexes relatively stable under air. Therefore, it is proposed to test the compound's OLED suitability.

Supplementary Materials: The following are available online at www.mdpi.com/xxx/s1, Experimental section, NMR spectra, IR spectra, crystal data tables of **2** (2017394), **3** (2017392), **4** (2017399), **5** (2017397), **6** (2017398), **7** (2017400), **8** (2017406), **9** (2017395), **11** (2017393), **14** (2017408), **15** (2017410), **16** (2017409), **17** (2017407) and **18** (2017411) and DFT calculations (PDF). Cartesian coordinates of calculated structures (XYZ).

Conflicts of Interest: The authors declare no competing financial interest.

References

1. Ramirez, F.; Desai, N.B.; Hansen, B.; McKelvie, N. Hexaphenylcarbodiphosphorane, $(C_6H_5)_3PCP(C_6H5)_3$. *J. Am. Chem. Soc.* **1961**, *83*, 3539–3540.
2. Tonner, R.; Frenking, G. Divalent Carbon(0) Chemistry, Part 1: Parent Compounds. Chem. – A Eur. J. 2008, 14, 3260–3272.
3. Tonner, R.; Frenking, G. Divalent Carbon(0) Chemistry, Part 2: Protonation and Complexes with Main Group and Transition Metal Lewis Acids. *Chem. – A Eur. J.* **2008**, *14*, 3273–3289.

4. Tonner, R.; Frenking, G. C(NHC)$_2$: Divalent Carbon(0) Compounds with N-Heterocyclic Carbene Ligands—Theoretical Evidence for a Class of Molecules with Promising Chemical Properties. *Angew. Chemie Int. Ed.* **2007**, *46*, 8695–8698.
5. Gernot Frenking; Tonner, R. Divalent carbon(0) compounds. *Pure Appl. Chem.* **2009**, *81*, 597–614.
6. Tonner, R.; Öxler, F.; Neumüller, B.; Petz, W.; Frenking, G. Carbodiphosphoranes: The Chemistry of Divalent Carbon(0). *Angew. Chemie Int. Ed.* **2006**, *45*, 8038–8042.
7. Appel, R.; Knoll, F.; Schöler, H.; Wihler, H.-D. Vereinfachte Synthese von Bis(triphenylphosphoranyliden)methan. *Angew. Chemie* **1976**, *88*, 769–770.
8. Sundermeyer, J.; Weber, K.; Peters, K.; von Schnering, H.G. Modeling Surface Reactivity of Metal Oxides: Synthesis and Structure of an Ionic Organorhenyl Perrhenate Formed by Ligand-Induced Dissociation of Covalent Re_2O_7. *Organometallics* **1994**, *13*, 2560–2562.
9. Petz, W.; Frenking, G. Carbodiphosphoranes and Related Ligands. In *Transition Metal Complexes of Neutral η^1-Carbon Ligands*; Springer-Verlag: Berlin, 2010; Vol. 30, pp. 49–92.
10. Petz, W. Addition compounds between carbones, CL2, and main group Lewis acids: A new glance at old and new compounds. *Coord. Chem. Rev.* **2015**, *291*, 1–27.
11. Gessner, V.H. *Modern Ylide Chemistry*; Gessner, V.H., Ed.; Springer International Publishing AG: Oxford, United Kingdom, 2018.
12. Kubo, K.; Jones, N.D.; Ferguson, M.J.; McDonald, R.; Cavell, R.G. Chelate and Pincer Carbene Complexes of Rhodium and Platinum Derived from Hexaphenylcarbodiphosphorane, Ph_3PCPPh_3. *J. Am. Chem. Soc.* **2005**, *127*, 5314–5315.
13. Cavell, R. G. Pincer and Chelate Carbodiphosphorane Complexes of Noble Metals In *The Chemistry of Pincer Compounds*; Morales-Morales, D., Jensen, C. M., Eds.; Elsevier Science: Amsterdam, 2007; Chapter 15, pp 347– 355.
14. Kubo, K.; Okitsu, H.; Miwa, H.; Kume, S.; Cavell, R.G.; Mizuta, T. Carbon(0)-Bridged Pt/Ag Dinuclear and Tetranuclear Complexes Based on a Cyclometalated Pincer Carbodiphosphorane Platform. *Organometallics* **2017**, *36*, 266–274.
15. Petz, W.; Neumüller, B.; Klein, S.; Frenking, G. Syntheses and Crystal Structures of $[Hg\{C(PPh_3)_2\}_2][Hg_2I_6]$ and $[Cu\{C(PPh_3)_2\}_2]I$ and Comparative Theoretical Study of Carbene Complexes $[M(NHC)_2]$ with Carbone Complexes $[M\{C(PH_3)_2\}_2]$ ($M = Cu^+, Ag^+, Au^+, Zn^{2+}, Cd^{2+}, Hg^{2+}$). *Organometallics* **2011**, *30*, 3330–3339.
16. Petz, W.; Neumüller, B. New platinum complexes with carbodiphosphorane as pincer ligand via ortho phenyl metallation. *Polyhedron* **2011**, *30*, 1779–1784.
17. Böttger, S.C.; Poggel Christina; Sundermeyer, J. Ortho-directed Dilithiation of Hexaphenyl-carbodiphosphorane. *Organometallics submitted*.
18. Stallinger, S.; Reitsamer, C.; Schuh, W.; Kopacka, H.; Wurst, K.; Peringer, P. Novel route to carbodiphosphoranes producing a new *P,C,P* pincer carbene ligand. *Chem. Commun.* **2007**, 510–512.
19. Reitsamer, C.; Schuh, W.; Kopacka, H.; Wurst, K.; Peringer, P. Synthesis and Structure of the First Heterodinuclear PCP−Pincer−CDP Complex with a Pd−Au d^8–d^{10} Pseudo-Closed-Shell Interaction. *Organometallics* **2009**, *28*, 6617–6620.
20. Reitsamer, C.; Schuh, W.; Kopacka, H.; Wurst, K.; Ellmerer, E.P.; Peringer, P. The First Carbodiphosphorane Complex with Two Palladium Centers Attached to the CDP Carbon: Assembly of a Single-Stranded di-Pd Helicate by the PCP Pincer ligand $C(dppm)_2$. *Organometallics* **2011**, *30*, 4220–4223.
21. Reitsamer, C.; Stallinger, S.; Schuh, W.; Kopacka, H.; Wurst, K.; Obendorf, D.; Peringer, P. Novel access to carbodiphosphoranes in the coordination sphere of group 10 metals: template synthesis and protonation of PCP pincer carbodiphosphorane complexes of $C(dppm)_2$. *Dalton Trans.* **2012**, *41*, 3503–3514.
22. Reitsamer, C.; Hackl, I.; Schuh, W.; Kopacka, H.; Wurst, K.; Peringer, P. Gold(I) and Gold(III) complexes of the $[CH(dppm)_2]^+$ and $C(dppm)_2$ PCP pincer ligand systems. *J. Organomet. Chem.* **2017**, *830*, 150–154.
23. Maser, L.; Herritsch, J.; Langer, R. Carbodiphosphorane-based nickel pincer complexes and their (de)protonated analogues: dimerisation, ligand tautomers and proton affinities. *Dalton Trans.* **2018**, *47*, 10544–10552.
24. Maser, L.; Vondung, L.; Langer, R. The ABC in pincer chemistry – From amine- to borylene- and carbon-based pincer-ligands. *Polyhedron* **2018**, *143*, 28–42.
25. Klein, M.; Xie, X.; Burghaus, O.; Sundermeyer, J. Synthesis and Characterization of a *N,C,N*-Carbodiphosphorane Pincer Ligand and Its Complexes. *Organometallics* **2019**, *38*, 3768–3777.
26. Su, W.; Pan, S.; Sun, X.; Zhao, L.; Frenking, G.; Zhu, C. Cerium–carbon dative interactions supported by carbodiphosphorane. *Dalton Trans.* **2019**, *48*, 16108–16114.

27. Adachi, C.; Hattori, R.; Kaji, H.; Tsujimura, T. *Handbook of Organic Light-Emitting Diodes*; 2018.
28. Yersin, H.; Czerwieniec, R.; Shafikov, M.Z.; Suleymanova, A.F.; Nozaki, K.; Iwamura, M.; Tsuboyama, A.; Osawa, M.; Hoshino, M.; Yu, R.; et al. Front Matter. *Highly Effic. OLEDs* 2018, i–xvi.
29. Deaton, J.C.; Switalski, S.C.; Kondakov, D.Y.; Young, R.H.; Pawlik, T.D.; Giesen, D.J.; Harkins, S.B.; Miller, A.J.M.; Mickenberg, S.F.; Peters, J.C. E-Type Delayed Fluorescence of a Phosphine-Supported $Cu_2(\mu\text{-}NAr_2)_2$ Diamond Core: Harvesting Singlet and Triplet Excitons in OLEDs. *J. Am. Chem. Soc.* **2010**, *132*, 9499–9508.
30. Leitl, M.J.; Zink, D.M.; Schinabeck, A.; Baumann, T.; Volz, D.; Yersin, H. Copper(I) Complexes for Thermally Activated Delayed Fluorescence: From Photophysical to Device Properties. *Top. Curr. Chem.* **2016**, *374*, 25.
31. Czerwieniec, R.; Leitl, M.J.; Homeier, H.H.H.; Yersin, H. Cu(I) complexes – Thermally activated delayed fluorescence. Photophysical approach and material design. *Coord. Chem. Rev.* **2016**, *325*, 2–28.
32. Yersin, H.; Czerwieniec, R.; Shafikov, M.Z.; Suleymanova, A.F. TADF Material Design: Photophysical Background and Case Studies Focusing on CuI and AgI Complexes. *ChemPhysChem* **2017**, *18*, 3508–3535.
33. Chen, X.-L.; Yu, R.; Zhang, Q.-K.; Zhou, L.-J.; Wu, X.-Y.; Zhang, Q.; Lu, C.-Z. Rational Design of Strongly Blue-Emitting Cuprous Complexes with Thermally Activated Delayed Fluorescence and Application in Solution-Processed OLEDs. *Chem. Mater.* **2013**, *25*, 3910–3920.
34. Gneuß, T.; Leitl, M.J.; Finger, L.H.; Yersin, H.; Sundermeyer, J. A new class of deep-blue emitting Cu(I) compounds - effects of counter ions on the emission behavior. *Dalton Trans.* **2015**, *44*, 20045–20055.
35. Gneuß, T.; Leitl, M.J.; Finger, L.H.; Rau, N.; Yersin, H.; Sundermeyer, J. A new class of luminescent Cu(I) complexes with tripodal ligands – TADF emitters for the yellow to red color range. *Dalton Trans.* **2015**, *44*, 8506–8520.
36. Volz, D.; Chen, Y.; Wallesch, M.; Liu, R.; Fléchon, C.; Zink, D.M.; Friedrichs, J.; Flügge, H.; Steininger, R.; Göttlicher, J.; et al. Bridging the Efficiency Gap: Fully Bridged Dinuclear Cu(I)-Complexes for Singlet Harvesting in High-Efficiency OLEDs. *Adv. Mater.* **2015**, *27*, 2538–2543.
37. Salehi, A.; Ho, S.; Chen, Y.; Peng, C.; Yersin, H.; So, F. Highly Efficient Organic Light-Emitting Diode Using A Low Refractive Index Electron Transport Layer. *Adv. Opt. Mater.* **2017**, *5*.
38. Igawa, S.; Hashimoto, M.; Kawata, I.; Yashima, M.; Hoshino, M.; Osawa, M. Highly Efficient Green Organic Light-emitting Diodes Containing Luminescent Tetrahedral Copper(I) Complexes. *J. Mater. Chem. C* **2013**, *1*, 542–551.
39. Hashimoto, M.; Igawa, S.; Yashima, M.; Kawata, I.; Hoshino, M.; Osawa, M. Highly Efficient Green Organic Light-Emitting Diodes Containing Luminescent Three-Coordinate Copper(I) Complexes. *J. Am. Chem. Soc.* **2011**, *133*, 10348–10351.
40. Zhang, Q.; Komino, T.; Huang, S.; Matsunami, S.; Goushi, K.; Adachi, C. Triplet Exciton Confinement in Green Organic Light-Emitting Diodes Containing Luminescent Charge-Transfer Cu(I) Complexes. *Adv. Funct. Mater.* **2012**, *22*, 2327–2336.
41. Czerwieniec, R.; Yu, J.; Yersin, H. Blue-Light Emission of Cu(I) Complexes and Singlet Harvesting. *Inorg. Chem.* **2011**, *50*, 8293–8301.
42. Chen, X.-L.; Yu, R.; Wu, X.-Y.; Liang, D.; Jia, J.-H.; Lu, C.-Z. A strongly greenish-blue-emitting Cu_4Cl_4 cluster with an efficient spin–orbit coupling (SOC): fast phosphorescence versus thermally activated delayed fluorescence. *Chem. Commun.* **2016**, *52*, 6288–6291.
43. Schinabeck, A.; Rau, N.; Klein, M.; Sundermeyer, J.; Yersin, H. Deep blue emitting Cu(I) tripod complexes. Design of high quantum yield materials showing TADF-assisted phosphorescence. *Dalton Trans.* **2018**, *47*, 17067–17076.
44. Lamansky, S.; Djurovich, P.; Murphy, D.; Abdel-Razzaq, F.; Lee, H.-E.; Adachi, C.; Burrows, P.E.; Forrest, S.R.; Thompson, M.E. Highly Phosphorescent Bis-Cyclometalated Iridium Complexes: Synthesis, Photophysical Characterization, and Use in Organic Light Emitting Diodes. *J. Am. Chem. Soc.* **2001**, *123*, 4304–4312.
45. Yersin, H.; Rausch, A.F.; Czerwieniec, R.; Hofbeck, T.; Fischer, T. The triplet state of organo-transition metal compounds. Triplet harvesting and singlet harvesting for efficient OLEDs. *Coord. Chem. Rev.* **2011**, *255*, 2622–2652.
46. Yersin, H. Triplet Emitters for OLED Applications. Mechanisms of Exciton Trapping and Control of Emission Properties. *Top. Curr. Chem.* **2004**, *241*, 1–26.
47. Yersin, H.; W. J. Finkenzeller Triplet Emitters for Organic Light-Emitting Diodes: Basic Properties. In: Highly Efficient OLEDs with Phosphorescent Materials; Yersin (Ed.), Wiley-VCH, Weinheim, Germany, 2008; 1–97.

48. Adachi, C.; Baldo, M.A.; Thompson, M.E.; Forrest, S.R. Nearly 100% internal phosphorescence efficiency in an organic light-emitting device. *J. Appl. Phys.* **2001**, *90*, 5048–5051.
49. Deaton, J.C.; Castellano, F.N. Archetypal Iridium(III) Compounds for Optoelectronic and Photonic Applications: Photophysical Properties and Synthetic Methods. in: E. Zysman- Colman (Ed.), Iridium(III) in Optoelectronic and Photonics Applications; Wiley Online Books; John Wiley and Sons, Chichester, UK, 2017; 1–69.
50. Liang, X.; Zhang, F.; Yan, Z.-P.; Wu, Z.-G.; Zheng, Y.; Cheng, G.; Wang, Y.; Zuo, J.-L.; Pan, Y.; Che, C.-M. Fast Synthesis of Iridium(III) Complexes Incorporating a Bis(diphenylphorothioyl)amide Ligand for Efficient Pure Green OLEDs. *ACS Appl. Mater. Interfaces* **2019**, *11*, 7184–7191.
51. Cheng, G.; Chow, P.-K.; Kui, S.C.F.; Kwok, C.-C.; Che, C.-M. High-Efficiency Polymer Light-Emitting Devices with Robust Phosphorescent Platinum(II) Emitters Containing Tetradentate Dianionic O∧N∧C∧N Ligands. *Adv. Mater.* **2013**, *25*, 6765–6770.
52. Li, G.; Fleetham, T.; Li, J. Efficient and Stable White Organic Light-Emitting Diodes Employing a Single Emitter. *Adv. Mater.* **2014**, *26*, 2931–2936.
53. Yersin, H.; Rausch, A.F.; Czerwieniec, R. Organometallic Emitters for OLEDs: Triplet Harvesting, Singlet Harvesting, Case Structures, and Trends. In *Physics of Organic Semiconductors*; Brütting, W., Adachi, C., Eds.; Wiley Online Books; 2013; pp. 371–424.
54. Baldo, M.A.; O'Brien, D.F.; You, Y.; Shoustikov, A.; Sibley, S.; Thompson, M.E.; Forrest, S.R. Highly efficient phosphorescent emission from organic electroluminescent devices. *Nature* **1998**, *395*, 151–154.
55. Che, C.-M.; Kwok, C.-C.; Lai, S.-W.; Rausch, A.F.; Finkenzeller, W.J.; Zhu, N.; Yersin, H. Photophysical Properties and OLED Applications of Phosphorescent Platinum(II) Schiff Base Complexes. *Chem. – A Eur. J.* **2010**, *16*, 233–247.
56. Williams, J.A.G. Photochemistry and Photophysics of Coordination Compounds: Platinum BT - Photochemistry and Photophysics of Coordination Compounds II. In; Balzani, V., Campagna, S., Eds.; Springer Berlin Heidelberg: Berlin, Heidelberg, 2007; pp. 205–268.
57. Murphy, L.; Williams, J.A.G. Luminescent Platinum Compounds: From Molecules to OLEDs BT - Molecular Organometallic Materials for Optics. In; Bozec, H., Guerchais, V., Eds.; Springer Berlin Heidelberg: Berlin, Heidelberg, 2010; pp. 75–111.
58. Cheng, G.; Kui, S.C.F.; Ang, W.-H.; Ko, M.-Y.; Chow, P.-K.; Kwong, C.-L.; Kwok, C.-C.; Ma, C.; Guan, X.; Low, K.-H.; et al. Structurally robust phosphorescent [Pt(O^N^C^N)] emitters for high performance organic light-emitting devices with power efficiency up to 126 lm W^{-1} and external quantum efficiency over 20%. *Chem. Sci.* **2014**, *5*, 4819–4830.
59. Cui, L.-S.; Nomura, H.; Geng, Y.; Kim, J.U.; Nakanotani, H.; Adachi, C. Controlling Singlet–Triplet Energy Splitting for Deep-Blue Thermally Activated Delayed Fluorescence Emitters. *Angew. Chemie Int. Ed.* **2017**, *56*, 1571–1575.
60. Samanta, P.K.; Kim, D.; Coropceanu, V.; Brédas, J.-L. Up-Conversion Intersystem Crossing Rates in Organic Emitters for Thermally Activated Delayed Fluorescence: Impact of the Nature of Singlet vs Triplet Excited States. *J. Am. Chem. Soc.* **2017**, *139*, 4042–4051.
61. Turro, N.J. *Modern Molecular Photochemistry of Organic Molecules.*; Turro, N.J., Ed.; Benjamin/Cummings: Melon Park, Ca, 1978.
62. Wang, H.M.J.; Chen, C.Y.L.; Lin, I.J.B. Synthesis, Structure, and Spectroscopic Properties of Gold(I)−Carbene Complexes. *Organometallics* **1999**, *18*, 1216–1223.
63. Matsumoto, K.; Matsumoto, N.; Ishii, A.; Tsukuda, T.; Hasegawa, M.; Tsubomura, T. Structural and spectroscopic properties of a copper(I)-bis(N-heterocyclic)carbene complex. *Dalton Trans.* **2009**, 6795–6801.
64. Krylova, V.A.; Djurovich, P.I.; Whited, M.T.; Thompson, M.E. Synthesis and characterization of phosphorescent three-coordinate Cu(i)-NHC complexes. *Chem. Commun.* **2010**, *46*, 6696–6698.
65. Catalano, V.J.; Munro, L.B.; Strasser, C.E.; Samin, A.F. Modulation of Metal--Metal Separations in a Series of Ag(I) and Intensely Blue Photoluminescent Cu(I) NHC-Bridged Triangular Clusters. *Inorg. Chem.* **2011**, *50*, 8465–8476.
66. Krylova, V.A.; Djurovich, P.I.; Aronson, J.W.; Haiges, R.; Whited, M.T.; Thompson, M.E. Structural and Photophysical Studies of Phosphorescent Three-Coordinate Copper(I) Complexes Supported by an N-Heterocyclic Carbene Ligand. *Organometallics* **2012**, *31*, 7983–7993.
67. Hamze, R.; Shi, S.; Kapper, S.C.; Muthiah Ravinson, D.S.; Estergreen, L.; Jung, M.-C.; Tadle, A.C.; Haiges, R.; Djurovich, P.I.; Peltier, J.L.; et al. "Quick-Silver" from a Systematic Study of Highly Luminescent, Two-Coordinate, d10 Coinage Metal Complexes. *J. Am. Chem. Soc.* **2019**, *141*, 8616–8626.

68. Shi, S.; Jung, M.C.; Coburn, C.; Tadle, A.; Sylvinson M. R., D.; Djurovich, P.I.; Forrest, S.R.; Thompson, M.E. Highly Efficient Photo- and Electroluminescence from Two-Coordinate Cu(I) Complexes Featuring Nonconventional N-Heterocyclic Carbenes. *J. Am. Chem. Soc.* **2019**, *141*, 3576–3588.
69. Hamze, R.; Peltier, J.L.; Sylvinson, D.; Jung, M.; Cardenas, J.; Haiges, R.; Soleilhavoup, M.; Jazzar, R.; Djurovich, P.I.; Bertrand, G.; et al. Eliminating nonradiative decay in Cu(I) emitters: >99% quantum efficiency and microsecond lifetime. *Science (80).* **2019**, *363*, 601–606.
70. Leitl, M.J.; Krylova, V.A.; Djurovich, P.I.; Thompson, M.E.; Yersin, H. Phosphorescence versus Thermally Activated Delayed Fluorescence. Controlling Singlet–Triplet Splitting in Brightly Emitting and Sublimable Cu(I) Compounds. *J. Am. Chem. Soc.* **2014**, *136*, 16032–16038.
71. Cordero, B.; Gómez, V.; Platero-Prats, A.E.; Revés, M.; Echeverría, J.; Cremades, E.; Barragán, F.; Alvarez, S. Covalent radii revisited. *Dalton Trans.* **2008**, 2832–2838.
72. Bondi, A. van der Waals Volumes and Radii. *J. Phys. Chem.* **1964**, *68*, 441–451.
73. Soloveichik, G.L.; Eisenstein, O.; Poulton, J.T.; Streib, W.E.; Huffman, J.C.; Caulton, K.G. Multiple structural variants of LnCuI(μ-X)$_2$CuILn (n = 1, 2). Influence of halide on a "soft" potential energy surface. *Inorg. Chem.* **1992**, *31*, 3306–3312.
74. Klein, M.; Sundermeyer, J. unpuplished.